

***Improved efficiency of PbS quantum dot sensitized NiO
photocathodes with naphthalene diimide electron acceptor bound to
the surface of the nanocrystals***

Mahfoudh Raissi,^{a†} Muhammad T. Sajjad,^{b†} Yoann Farré,^a Thomas Roland,^b Arvydas Ruseckas,^b Ifor D. W. Samuel,^{*b} Fabrice Odobel^{*a}

†these two persons equally participate to the work

^a*CEISAM, Chimie Et Interdisciplinarité, Synthèse, Analyse, Modélisation, CNRS, UMR CNRS 6230, UFR des Sciences et des Techniques ; 2, rue de la Houssinière - BP 92208; 44322 NANTES Cedex 3 (France)*

E-mail: Fabrice.Odobel@univ-nantes.fr

^b*Organic Semiconductor Centre, SUPA, School of Physics and Astronomy, University of St Andrews, North Haugh, St Andrews, Fife, (United Kingdom).*

E-mail: idws@st-andrews.ac.uk

Abstract

Hybrid materials combining a wide bandgap metal oxide semiconductor, metal chalcogenide nanocrystals and molecular systems represent very attractive materials for fabricating devices with new function or improved photoelectrochemical performances. This study deals with sensitization of NiO, which is a p-type semiconductor, by quantum dots (QDs) of PbS with an average diameter of 3 nm. The PbS QDs were attached to the monocrystalline film of NiO by mercaptopropionic acid linker and were subsequently capped with methyl-pyridine naphthalene diimide (NDI) units to prepare quantum dot sensitized solar cells (p-QDSSCs) on NiO electrodes. Time-resolved photoluminescence measurements of the PbS emission were used to determine the rate constants for charge transfer from the PbS exciton to the NiO, cobalt based redox mediator and NDI. Notably, it was shown that NDI quenches the PbS exciton by electron transfer with a quite fast rate constant ($6.9 \times 10^7 \text{ s}^{-1}$). The PbS QDs sensitized NiO films were finally used to fabricate solar cells with *tris*(4,4'-ditert-butyl-2,2'-bipyridine) cobalt(III/II) as redox mediator. It was observed that the presence of NDI on PbS improved the photovoltaic performance by 50% relative to that of cells without NDI, leading to a device with the following characteristics: $J_{sc} = 5.75 \text{ mA/cm}^2$, $V_{oc} = 226 \text{ mV}$, $ff = 34\%$ and $PCE = 0.44\%$. This study demonstrates that photogalvanic processes can be a productive pathway to better performing sensitized p-type semiconductor for p-QDSSC. In other words, photoinduced electron transfer from the QDs

towards the electrolyte rather than initial photoinduced charge injection into the p-type semiconductor can be a favorable operative mechanism in QD sensitized NiO films and might be exploited further for the construction of better performing solar cells or photocatalytic devices.

Introduction

The combination of quantum dots (QDs), molecules and wide bandgap nanocrystalline semiconductors offers many exciting opportunities for the fabrication of hybrids systems for photovoltaic and photoelectrosynthetic solar cells (DSPECs). Metal chalcogenide quantum dots have been successfully implemented as light collectors in p-type dye sensitized solar cells (p-DSSCs).[1-12] Recently, we have been very interested in PbS quantum dots for p-DSSCs owing to their significant efficiencies making them valuable materials to consider to fabricate photocathodes.[13] Moreover, PbS QDs display high absorbance in the near-infrared,[14] they can potentially exhibit multiple exciton generation,[15] they have longer excited state lifetimes than CdSe or CdS QDs and they are easily prepared from cheap starting materials.[16, 17] These properties make PbS QDs potentially very attractive for photovoltaic[18-20] or photocatalytic applications,[21] which is validated with the high power conversion efficiencies recently reported with solar cells made with PbS QDs.[22] The association of catalyst[23] and even enzymes[24] with QDs has already led to efficient photocatalytic reactors with unique properties.[25, 26] The combination of NiO photocathode for hydrogen production in DSPECs was also demonstrated with very promising performance and stability.[27-30] Moreover, in this context, interfacial electron transfer (ET) from photoexcited QDs to a surface attached molecular acceptor has been investigated in recent years.[31-36] For instance, with PbS QDs, the ultrafast dissociation of the exciton created on the QDs by quinone derivatives,[37, 38] fullerene derivatives,[39] methylene blue[40] and porphyrin[41] acting as electron acceptors has been clearly demonstrated in recent studies.

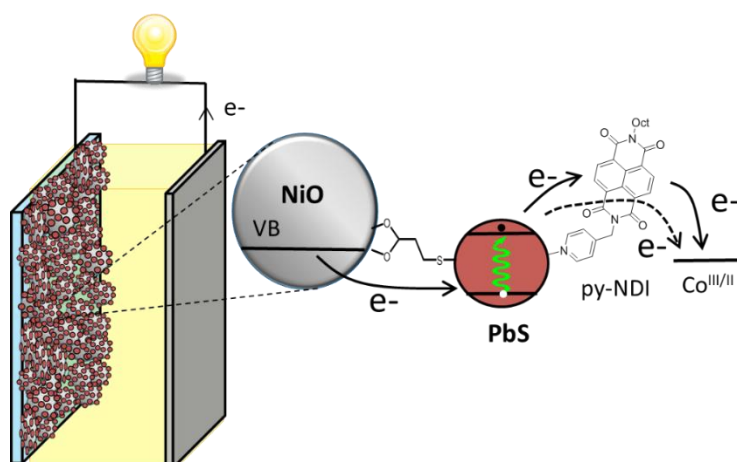


Chart 1. Schematic representation of the solar cell prepared in this study and structure of the organic ligand py-NDI.

On the other hand, it has also been established that charge recombination reactions play a major role in p-DSSCs and therefore different strategies have to be developed to circumvent this energy wasting process.[42-44] Notably, the introduction of a secondary electron acceptor on the dye that can increase the distance with hole in NiO represent a fruitful strategy.[45-48] These considerations prompted us to combine a second electron acceptor such as naphthalene diimide (NDI) with PbS quantum dots immobilized on a nanocrystalline NiO electrode (Chart 1). We have chosen NDI as electron acceptor because: i) the reduction potential of NDI is well positioned to accept an electron from PbS conduction band (CB); ii) it displays higher lying excited states than the PbS bandgap precluding quenching by energy transfer and iii) it was previously demonstrated that NDI is an effective relay to transfer electron from the sensitizer to the cobalt complex used here as redox mediator.[42, 46, 49-51] Towards this objective, we demonstrate in this study that the post-functionalization of PbS quantum dots by py-NDI ligand, which acts as an electron acceptor in the electron transfer chain from NiO valence band to the NDI unit until the redox couple, improves the photovoltaic performances of the p-DSSC solar cells by about 50%. The enhanced photovoltaic efficiency was rationalized by a time resolved photoluminescence study which revealed that oxidative quenching of PbS excitons is accelerated by the NDI acceptor facilitating electron transfer to the redox mediator in the electrolyte. Overall, an increase of 50% of the photoconversion efficiency of the p-QDSSc was gained after the introduction of py-NDI on the surface of the PbS quantum dots.

Results and discussion

Preparation of the hybrid system: NiO/MPA/PbS/py-NDI

The synthesis of the py-NDI molecule was readily accomplished in two steps from commercially available reagents and is described in detail in supporting information. A colloidal solution of PbS quantum dots (diameter 3.0 nm) was prepared following the hot injection methodology initially developed by Hines and Scholes.[16] The oleic acid capped PbS nanocrystals (PbS-OA) were subsequently treated by a solution of tetrabutylammonium iodide (TBAI) to passivate the trap states, which are known to quench the exciton of PbS and therefore to decrease the exciton lifetime and consequently the charge injection quantum yield.[18, 22, 52, 53] Herein, the quantum dots have an average diameter of 3.0 nm, a band-edge absorption peak centered at 945 nm in toluene solution and a photoluminescence peak centered at 1063 nm in solution (Figure S1). The PbS QDs were subsequently grafted on the nanocrystalline NiO films with the well-known linker assisted methodology using mercaptopropionic acid (MPA) as a linker.[18, 54, 55] The NiO electrode was first dipped in a solution of MPA and then rinsed, then in a colloidal solution of PbS preliminarily treated

with TBAI (PbS-TBAI) to passivate the trap states arising from dangling bonds.[52, 53, 56] A second treatment with a cetyl trimethyl ammonium bromide (CTAB) solution was essential to decrease the oleate ligands concentration around the nanocrystal in order to reduce the footprint of the QD on the NiO surface thus enabling a closer QD packing of the nanocrystals.[13]

The preparation of the NiO photoelectrode follows a procedure that we had previously reported.[13, 57] Briefly, the electrode consists of FTO glass on which a compact layer of NiO was first deposited to ensure a stronger binding of the nanoparticles of NiO and to prevent the interfacial charge recombination with the redox shuttle in the electrolyte.[47, 58] A layer of nanoparticles of NiO was deposited by screen printing and then sintered at 400°C. The mesoporous film was finally soaked in a solution of nickel acetate, and then annealed at 200°C. This treatment is known to increase the particle necking and to decrease the concentration of recombination sites on NiO surface.[59]

It is known that pyridine binds to QDs and can act as a ligand of PbS.[60, 61] Accordingly, the above prepared PbS sensitized NiO film was soaked in a solution of py-NDI for two hours in order to attach the ligand to the PbS nanocrystal. The absorption spectra of the NiO photoelectrode before and after immobilization of the adsorbate py-NDI on the PbS surface reveal that the ligand does not induce perceptible modification.

Energetic considerations of the charge transfer processes

To shed some light on the operation principle of the solar cell and to elucidate the potential charge transfer reactions between the components, it is important to determine their thermodynamic feasibility. The valence band (VB) and conduction band (CB) potentials of the PbS quantum dots used herein were previously determined by electrochemistry.[57] The prepared PbS quantum dot has a diameter of 3.0 nm, corresponding to a band gap of 1.34 eV and display a VB and a CB potential lying respectively at 0.48 V vs SCE and -0.7 V vs SCE. The reduction potential of py-NDI ($E_{\text{Red}}(\text{NDI}/\text{NDI}^-)$) was recorded by cyclic voltammetry in acetonitrile (Figure S2) and was found to be located at -0.46 V vs. SCE and its oxidation potential is located outside the electrochemical window of our experimental conditions ($E_{\text{Ox}} > 1.6$ V vs. SCE).

As a result, one can calculate the Gibbs free energy of the electron transfer from the PbS exciton to NDI (ΔG_{ET}) from the equation:

$$\Delta G_{\text{ET}} = E_{\text{CB}}(\text{PbS}) - E_{\text{Red}}(\text{NDI}/\text{NDI}^-)$$

using the above values, the electron transfer from PbS exciton is an exothermic process ($\Delta G_{\text{ET}} = -0.24$ eV).

Quenching by energy transfer from photoexcited PbS nanocrystal to NDI can be confidently ruled out because the singlet ($E_S(^1\text{NDI}^*) = 3.3 \text{ eV}$)[62] and the triplet ($E_S(^3\text{NDI}^*) = 2.03 \text{ eV}$)[62] of NDI excited states lie much above that of the PbS exciton (1.34 eV). Oxidative quenching of the PbS exciton by py-NDI, that is a hole transfer from VB of PbS to the occupied molecular orbital of NDI producing an oxidized NDI^+ and an electron residing in the conduction band (CB) of PbS can be discounted because this process is endothermic ($\Delta G = E_{\text{Ox}}(\text{NDI}) - E_{\text{VB}}(\text{PbS}) \gg 1 \text{ eV}$). As a result, the only process that could be responsible of a reduced lifetime of PbS emission is electron transfer to NDI leading to PbS^+/NDI .

Photophysical study

Basically, the operation principle of the solar cell can follow two distinct sequences: i) first, dissociation of the PbS exciton by hole injection into the VB of NiO followed by an electron shift from the reduced PbS to NDI and finally a second electron transfer to the Co(III) complex (path A in Figure 2) or ii) an initial electron transfer to the NDI by the photoexcited PbS to form the reduced NDI and a hole in the VB of PbS. This first step is followed by a hole shift from the VB of PbS to that of NiO and the reduction of the Co(III) complex with the reduced NDI or *vice versa* (path B in Figure 2).

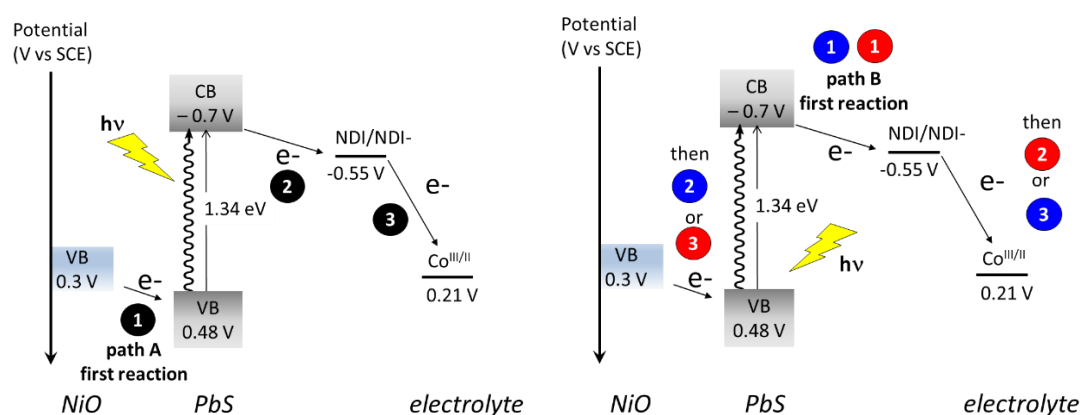


Figure 2. Diagram showing the pertinent states of each component and the two potential pathways (A left or B right see text) involved in the solar cell operation principle. The number inside the disk indicates the order of the process in the charge transfer chain from NiO VB to the Co(III).

A photophysical study by time-resolved photoluminescence was conducted to shed some light on the rate constants of the charge transfer processes occurring after light excitation of the PbS QD. Towards this goal, the luminescence lifetime of PbS QD was recorded in different environments by time resolved spectroscopy with a Hamamatsu infrared streak camera with femtosecond pulse excitation of PbS at 640 nm. The first measurements were performed on PbS QDs grafted on mesoporous alumina film, an oxide for which no charge transfer is thermodynamically allowed

because the VB and CB of Al_2O_3 are located too far apart from those of PbS. The photoluminescence decay was monitored with the electrolyte lacking the redox couple (propylene carbonate+ LiClO_4) to provide the reference lifetime of PbS emission without quencher and then with the ligand py-NDI connected to PbS in order to determine the quenching rate of the photoinduced electron transfer from PbS^* to NDI in the absence and in the presence of the oxidized species of the redox shuttle (Co(III/II) complex). In a second time, the lifetime measurements were conducted on the NiO films with plain PbS with and without py-NDI and in the presence and in the absence of the Co (III/II) complex in the electrolyte solution. Figure 3 (left panel) illustrates the luminescence decay profiles of PbS QDs in the absence and in the presence of py-NDI, both on Al_2O_3 and NiO and with or without the cobalt redox mediator. As shown extensively before for QDs attached to nanocrystalline SC surfaces, the decays cannot be fitted with a single exponential function and they were analyzed using a multiexponential function, and the average lifetimes, $\langle\tau\rangle$, were evaluated.[8, 12, 36, 40, 57]

However, in our study the time dependent rate constants of the luminescence quenching for each environment were determined following procedure similar reported previously[12, 57] i.e. by differentiating the natural logarithm of the PL ratio QDs with and without quencher (shown in Figure 3) as :

$$k_{CT}(t) = -\frac{d}{dt} \left(\text{Ln} \left(\frac{\text{PL of QD with acceptor}}{\text{PL of QD on Al}_2\text{O}_3} \right) \right)$$

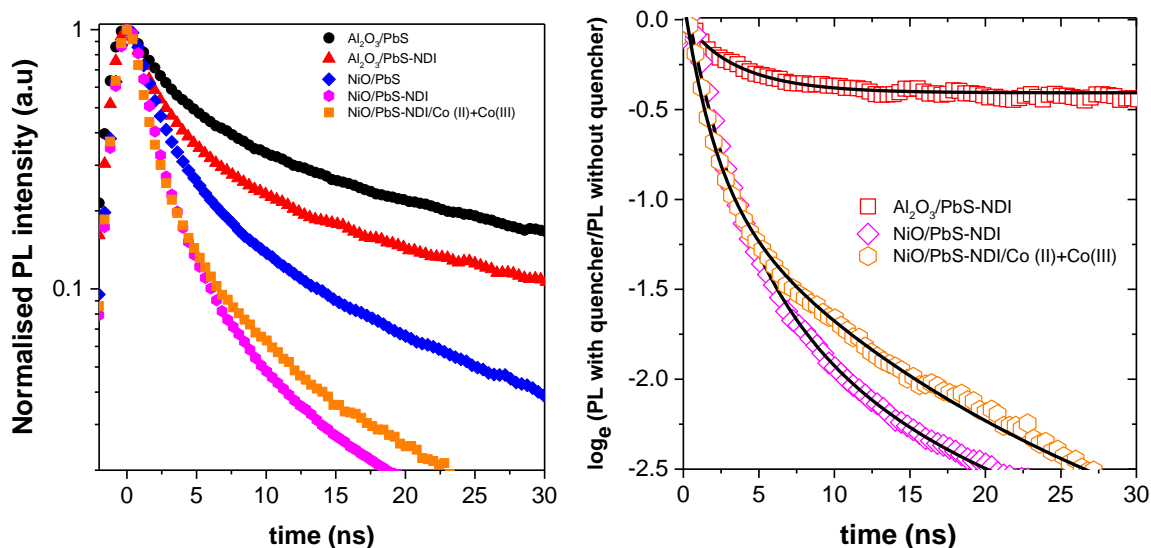


Figure 3. (left panel) Normalized photoluminescence decays of the PbS ($d=3.0$ nm) recorded in different environments. (right panel) Ratio of photoluminescence kinetics of the 3.0 nm PbS QDs with quencher (electron/hole acceptor) to photoluminescence kinetics without quencher (i.e on alumina). The solid black lines are fits to PL decays. The slope of natural logarithm of PL ratio is k_{CT} .

The PL ratio shown in Figure 3 (right panel) was fitted with three exponentials before differentiation. The resultant time dependent rate constants obtained from differentiation of natural logarithm of PL ratios are shown in Figure 4. An average charge transfer rate determined using the equation below is summarized in Table 1.

$$\langle k_{CT} \rangle = \frac{1}{\tau_1} \int_0^{\tau_1} k_{CT}(t) dt$$

where τ_1 corresponds to time for the fluorescence decay to fall to 1/e of its initial value. The obtained numbers are gross simplification of the time dependent behaviour seen in Figure 4, therefore care should be taken using these numbers.

The shortening of the photoluminescence of PbS in the presence of py-NDI on Al₂O₃ and on NiO accounts for the oxidative quenching of the QD by electron transfer leading to PbS⁺/NDI⁻ as it is the sole deactivation thermodynamically allowed on Al₂O₃ (see above). Interestingly, the photoinduced electron transfer from PbS* to NDI is quite fast in spite of being slower by a factor of 2.5 than hole injection (Table 1).

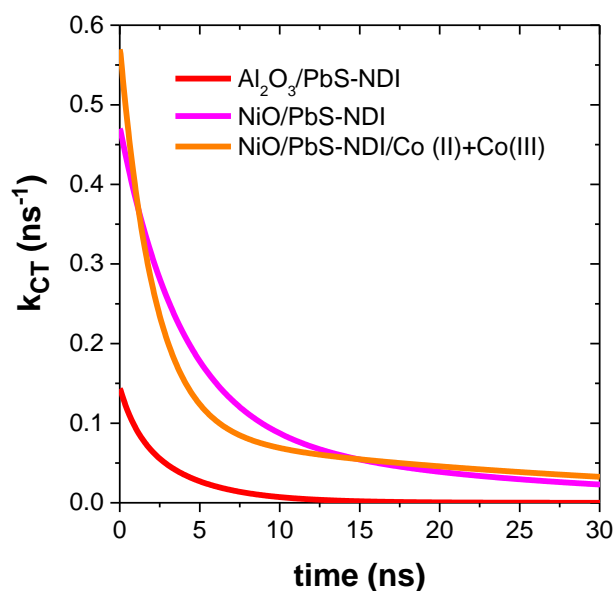


Figure 4. Charge transfer rate constants determined by differentiating the logarithm of PL ratios (given in Figure 3 right panel).

Table 1. Average Rate constants of photoluminescence quenching reaction from PbS exciton. $\langle k_{red} (s^{-1}) \rangle$ is the rate of photoinduced electron transfer (reduction) to Co(II)+ Co(III) , $\langle k_{inj} (s^{-1}) \rangle$ is the rate constant for hole injection to NiO and $\langle k_{inj+red} (s^{-1}) \rangle$ is the combined rate constants for both electron and hole transfer to NiO and Co(II)+ Co(III).

	Quencher	$\langle \text{rate} (s^{-1}) \rangle$
on Al ₂ O ₃	none ^a	1.5×10^7
	Co(II)+Co(III)	1.3×10^8
	py-NDI	6.9×10^7
	py-NDI + Co(II)+Co(III)	2.0×10^8
on NiO	none ^a	1.7×10^8
	Co(II)+Co(III)	2.5×10^8
	py-NDI	3.8×10^8
	py-NDI + Co(II)+Co(III)	4.0×10^8

^anone means that the photocathode is only in contact with the neutral electrolyte, that is a solution of LiClO₄ in propylene carbonate.

In our previous study, we have shown that PbS excitons in NiO based p-DSSC dissociate both by hole injection into NiO and oxidative quenching by the Co(III) complex.[57] It is important to note that the adsorption of py-NDI increases the oxidative quenching of the PbS exciton as its lifetime is systematically shortened in the presence of py-NDI even though all other conditions were kept constant (Table1). In summary we find that NDI bound to PbS quenches the exciton with a significant average rate constant ($6.9 \times 10^7 s^{-1}$) by electron transfer to form NDI⁻ both on Al₂O₃ and NiO.

Photovoltaic performances in p-QDSSC

The photovoltaic properties of the PbS sensitized NiO film were assessed in sealed sandwich solar cells consisting of a platinum counter electrode with the complexes *tris*(4,4'-ditert-butyl-2,2'-bipyridine) cobalt(III/II) as redox couple (the structure of the complex is given in Figure S3). We have previously demonstrated that the latter electrolyte proved to be well-suited for NiO p-DSSC sensitized with PbS QDs.[13, 57] The solar cells were prepared with NiO photocathodes coated with PbS QDs treated with py-NDI and they were compared to solar cells without adsorbate (Table 2). Naturally, all the cells were fabricated using exactly the same procedure apart from the final treatment with the py-NDI component. The performance of the solar cells is shown in Table 2 and the photoaction (Incident photon-to-current efficiency (IPCE) as a function of incident wavelength) and current/voltage characteristics are shown in Figure 5. The data in Table 2 correspond to the average values of several measurements made on independent solar cells.

Table 2. Photovoltaic performances of NiO-based p-QDSSCs recorded under simulated solar light AM1.5 (100 mW/cm²).

cell	V _{OC} (mV)	J _{SC} (mA.cm ⁻²)	ff (%)	PCE (%)
without py-NDI	5.05 (±0.15)	181 (±7)	32 (±1)	0.29 (±0.02)
with py-NDI	5.75 (±0.15)	226 (±1)	34 (±1)	0.44 (±0.01)

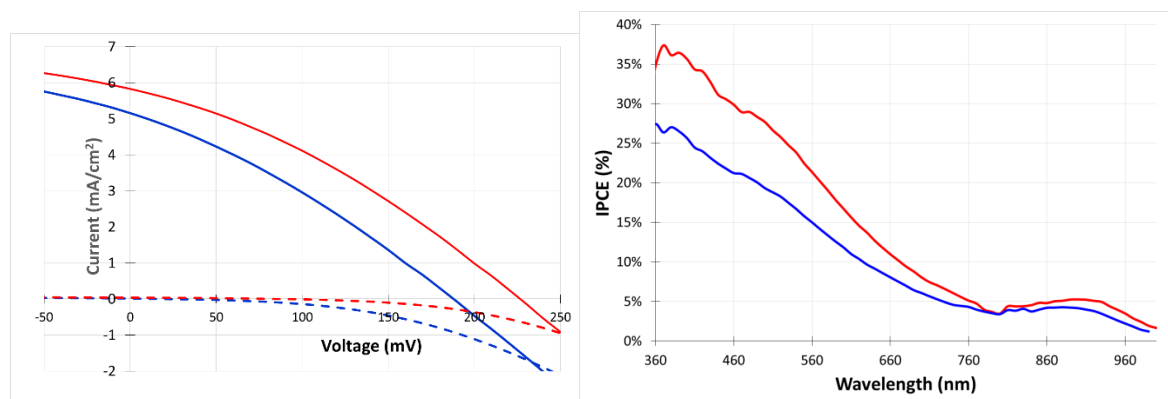


Figure 5. Current/voltage characteristics recorded in the dark (dash line) and under simulated sunlight (plain line) and photoaction spectra of the cell without **py-NDI** (blue) and with **py-NDI** (red).

In Table 2 and Figure 5 show that presence of py-NDI the J_{sc} and the V_{oc} are both enhanced relative to the reference cell (without py-NDI) leading to an overall increase of the PCE of 50%. The increased IPCE with **py-NDI** reflects a higher injection quantum efficiency or a better charge collection efficiency. Indeed, the absorbance of the cells was not modified therefore the light harvesting efficiency was not significantly raised. NDI could adsorb on NiO surface *via* the pyridyl group, but a significant contribution of NDI to photocurrent density *via* direct hole injection from NDI excited state can be rule out because of several reasons. First, NDI excited state is very short-lived[63] and taking into account that this dye is electronically deconjugated to the pyridine moiety (methylene spacer), the hole injection is most certainly inefficient. Second, the absorption spectrum of **py-NDI** (Figure S4) demonstrates that NDI absorbs below 400 nm and display very sharp absorption bands (359 and 381 nm). If NDI would have significantly contribution to the photocurrent density of the cell, the IPCE spectrum would have featured these two bands, which is not the case (Figure 5). Finally, we can see that the IPCE spectrum of the cell with **py-NDI** is, within experimental error, a linear combination of the IPCE spectrum without **py-NDI** or that of the absorption spectrum of PbS (see Figure S1). Moreover, the IPCE spectrum of the cell with py-NDI presents a clear amplification where NDI does not absorb at all, these are on the excitonic peak of PbS (900 nm) and between 400-700 nm. In a previous study, we have shown that the electron transfer from the CB of PbS to the cobalt

electrolyte was a limiting step[57] owing to the slow electron shift to the cobalt(III) complex owing to the large reorganization energy[64] and probably to the presence of surface defects (dangling bonds) that trap the electron. Based on the above time-resolved photoluminescence study, it is clear that the major consequence of the presence of py-NDI is the acceleration of oxidative quenching of PbS*. In other words, one main feature of py-NDI is to increase the quantum efficiency of electron transfer between PbS and the electrolyte. Moreover, NDI most probably retards charge recombination, since the electron generated on PbS upon hole injection (path A) is transferred to the NDI.

From the results of the photophysical study and those of the photovoltaic measurements, we can therefore conclude that the oxidative quenching of PbS excitons (path B in Figure 2) is a favorable pathway for electricity production, since an enhancement of this process induces a higher photovoltage and photocurrent density. Consequently, this finding provides new insight into the mechanism of the interfacial charge transfer in p-DSSC and can potentially contribute to the development of better performing QD-based sensitized devices for both photovoltaic and photocatalysis. Indeed, galvanic process could be exploited in the future to direct the electron either to other electron acceptors or catalysts grafted on the QDs while enhancing the overall efficiency of the photoelectrochemical device.

Conclusion

In this work, we have investigated the impact on solar cell efficiency of a molecular electron acceptor such as py-NDI in PbS sensitized NiO p-DSSC and demonstrated the positive impact on solar cell performances. Using time-resolved emission spectroscopy we have shown that NDI oxidatively quenches the PbS exciton resulting in a better performing solar cell with 50% improved efficiency. The enhanced performance is attributed to a higher electron transfer efficiency to the cobalt electrolyte and most probably a slow charge recombination upon electron shift to NDI. In addition this study unequivocally demonstrates that galvanic process can be a productive pathway to better performing sensitized p-type semiconductors for DSSC and DSPEC. Our approach of post-modification of the QDs by a functional ligand after their immobilization on the NiO surface allows a rapid screening of many components such as other electron acceptors or electrocatalyst with minimum synthetic effort. We believe that these findings represent valuable information for the future design of QD sensitized p-DSSC and p-DSPECs.

Acknowledgements

ANR is gratefully acknowledged for the financial support of these researches through the “QuePhelec” project (n° ANR-13-BS10-0011-01). Région des Pays de la Loire and Nantes University for the project LUMOMAT are also acknowledged. We acknowledge support from the European Research

Council (grant number 321305) and the EPSRC (grant number EP/L017008/1). IDWS is a Royal Society Wolfson Research Merit award holder.

References

- [1] I. Barcelo, E. Guillen, T. Lana-Villarreal, R. Gomez, Preparation and Characterization of Nickel Oxide Photocathodes Sensitized with Colloidal Cadmium Selenide Quantum Dots. *J. Phys. Chem. C* 117 (2013) 22509-22517.
- [2] Y. Na, B. Hu, Q.-L. Yang, J. Liu, L. Zhou, R.-Q. Fan, Y.-L. Yang, CdS quantum dot sensitized p-type NiO as photocathode with integrated cobaloxime in photoelectrochemical cell for water splitting. *Chin. Chem. Lett.* 26 (2015) 141-144.
- [3] F. Safari-Alamuti, J. R. Jennings, M. A. Hossain, L. Y. L. Yung, Q. Wang, Conformal growth of nanocrystalline CdX (X = S, Se) on mesoscopic NiO and their photoelectrochemical properties. *Phys. Chem. Chem. Phys.* 15 (2013) 4767-4774.
- [4] P. Meng, M. Wang, Y. Yang, S. Zhang, L. Sun, CdSe quantum dots/molecular cobalt catalyst co-grafted open porous NiO film as a photocathode for visible light driven H₂ evolution from neutral water. *J. Mater. Chem. A* 3 (2015) 18852-18859.
- [5] M.-A. Park, S.-Y. Lee, J.-H. Kim, S.-H. Kang, H. Kim, C.-J. Choi, K.-S. Ahn, CdSe Quantum Dot-sensitized, Nanoporous p-type NiO Photocathodes for Quantum Dot-sensitized Solar Cells. *Mol. Cryst. Liq. Cryst.* 598 (2014) 154-162.
- [6] M.-A. Park, S.-Y. Lee, J.-H. Kim, S.-H. Kang, H. Kim, C.-J. Choi, K.-S. Ahn, Enhanced photoelectrochemical response of CdSe quantum dot-sensitized p-type NiO photocathodes. *Phys. Status Solidi A* 211 (2014) 1868-1872.
- [7] X. Wu, E. K. L. Yeow, Charge-transfer processes in single CdSe/ZnS quantum dots with p-type NiO nanoparticles. *Chem. Commun.* 46 (2010) 4390-4392.
- [8] K. Zheng, K. Židek, M. Abdellah, W. Zhang, P. Chábera, N. Lenngren, A. Yartsev, T. Pullerits, Ultrafast Charge Transfer from CdSe Quantum Dots to p-Type NiO: Hole Injection vs Hole Trapping. *J. Phys. Chem. C* 118 (2014) 18462-18471.
- [9] J. H. Rhee, Y. H. Lee, P. Bera, S. I. Seok, Cu₂S-deposited mesoporous NiO photocathode for a solar cell. *Chem. Phys. Lett.* 477 (2009) 345-348.
- [10] C. Zhao, X. Zou, S. He, CdTeO₃ deposited mesoporous NiO photocathode for a solar cell. *J. Nanomater.* (2014) 372381/372381-372381/372386, 372386 pp.
- [11] T. J. Macdonald, Y. J. Mange, M. R. Dewi, H. U. Islam, I. P. Parkin, W. M. Skinner, T. Nann, CuInS₂/ZnS nanocrystals as sensitizers for NiO photocathodes. *J. Mater. Chem. A* 3 (2015) 13324-13331.
- [12] J. Park, M. T. Sajjad, P.-H. Jouneau, A. Ruseckas, J. Faure-Vincent, I. D. W. Samuel, P. Reiss, D. Aldakov, Efficient eco-friendly inverted quantum dot sensitized solar cells. *J. Mater. Chem. A* 4 (2016) 827-837.
- [13] M. Raissi, Y. Pellegrin, S. Jobic, M. Boujtita, F. Odobel, Infra-red photoresponse of mesoscopic NiO-based solar cells sensitized with PbS quantum dot. *Scientific Reports* abbreviation *Sci. Rep.* 6 (2016) doi: 10.1038/srep24908.
- [14] L. Cademartiri, E. Montanari, G. Calestani, A. Migliori, A. Guagliardi, G. A. Ozin, Size-Dependent Extinction Coefficients of PbS Quantum Dots. *J. Am. Chem. Soc.* 128 (2006) 10337-10346.
- [15] J. B. Sambur, T. Novet, B. A. Parkinson, Multiple Exciton Collection in a Sensitized Photovoltaic System. *Science* 330 (2010) 63-66.
- [16] M. A. Hines, G. D. Scholes, Colloidal PbS Nanocrystals with Size-Tunable Near-Infrared Emission: Observation of Post-Synthesis Self-Narrowing of the Particle Size Distribution. *Adv. Mater.* 15 (2003) 1844-1849.
- [17] J. Zhang, R. W. Crisp, J. Gao, D. M. Kroupa, M. C. Beard, J. M. Luther, Synthetic Conditions for High-Accuracy Size Control of PbS Quantum Dots. *J. Phys. Chem. Lett.* 6 (2015) 1830-1833.
- [18] G. H. Carey, A. L. Abdelhady, Z. Ning, S. M. Thon, O. M. Bakr, E. H. Sargent, Colloidal Quantum Dot Solar Cells. *Chem. Rev.* 115 (2015) 12732-12763.

- [19] G.-H. Kim, F. P. García de Arquer, Y. J. Yoon, X. Lan, M. Liu, O. Voznyy, Z. Yang, F. Fan, A. H. Ip, P. Kanjanaboos, S. Hoogland, J. Y. Kim, E. H. Sargent, High-Efficiency Colloidal Quantum Dot Photovoltaics via Robust Self-Assembled Monolayers. *Nano Lett.* 15 (2015) 7691-7696.
- [20] H. Wang, T. Kubo, J. Nakazaki, T. Kinoshita, H. Segawa, PbS-Quantum-Dot-Based Heterojunction Solar Cells Utilizing ZnO Nanowires for High External Quantum Efficiency in the Near-Infrared Region. *J. Phys. Chem. Lett.* 4 (2013) 2455-2460.
- [21] R. Trevisan, P. Rodenas, V. Gonzalez-Pedro, C. Sima, R. S. Sanchez, E. M. Barea, I. Mora-Sero, F. Fabregat-Santiago, S. Gimenez, Harnessing Infrared Photons for Photoelectrochemical Hydrogen Generation. A PbS Quantum Dot Based “Quasi-Artificial Leaf”. *J. Phys. Chem. Lett.* 4 (2013) 141-146.
- [22] X. Lan, O. Voznyy, F. P. García de Arquer, M. Liu, J. Xu, A. H. Proppe, G. Walters, F. Fan, H. Tan, M. Liu, Z. Yang, S. Hoogland, E. H. Sargent, 10.6% Certified Colloidal Quantum Dot Solar Cells via Solvent-Polarity-Engineered Halide Passivation. *Nano Lett.* 16 (2016) 4630-4634.
- [23] J. Huang, K. L. Mulfort, P. Du, L. X. Chen, Photodriven Charge Separation Dynamics in CdSe/ZnS Core/Shell Quantum Dot/Cobaloxime Hybrid for Efficient Hydrogen Production. *J. Am. Chem. Soc.* 134 (2012) 16472-16475.
- [24] K. A. Brown, S. Dayal, X. Ai, G. Rumbles, P. W. King, Controlled Assembly of Hydrogenase-CdTe Nanocrystal Hybrids for Solar Hydrogen Production. *J. Am. Chem. Soc.* 132 (2010) 9672-9680.
- [25] M. Wang, K. Han, S. Zhang, L. Sun, Integration of organometallic complexes with semiconductors and other nanomaterials for photocatalytic H₂ production. *Coord. Chem. Rev.* 287 (2015) 1-14.
- [26] F. Wen, C. Li, Hybrid Artificial Photosynthetic Systems Comprising Semiconductors as Light Harvesters and Biomimetic Complexes as Molecular Cocatalysts. *Acc. Chem. Res.* 46 (2013) 2355-2364.
- [27] B. Liu, X.-B. Li, Y.-J. Gao, Z.-J. Li, Q.-Y. Meng, C.-H. Tung, L.-Z. Wu, A solution-processed, mercaptoacetic acid-engineered CdSe quantum dot photocathode for efficient hydrogen production under visible light irradiation. *Energy Environ. Sci.* 8 (2015) 1443-1449.
- [28] Y. Dong, R. Wu, P. Jiang, G. Wang, Y. Chen, X. Wu, C. Zhang, Efficient Photoelectrochemical Hydrogen Generation from Water Using a Robust Photocathode Formed by CdTe QDs and Nickel Ion. *ACS Sustain. Chem. Eng.* 3 (2015) 2429-2434.
- [29] H. B. Yang, J. Miao, S.-F. Hung, F. Huo, H. M. Chen, B. Liu, Stable Quantum Dot Photoelectrolysis Cell for Unassisted Visible Light Solar Water Splitting. *ACS Nano* 8 (2014) 10403-10413.
- [30] T. P. A. Ruberu, Y. Dong, A. Das, R. Eisenberg, Photoelectrochemical Generation of Hydrogen from Water Using a CdSe Quantum Dot-Sensitized Photocathode. *ACS Catal.* (2015) 2255-2259.
- [31] A. J. Morris-Cohen, M. D. Peterson, M. T. Frederick, J. M. Kamm, E. A. Weiss, Evidence for a Through-Space Pathway for Electron Transfer from Quantum Dots to Carboxylate-Functionalized Viologens. *J. Phys. Chem. Lett.* 3 (2012) 2840-2844.
- [32] A. J. Morris-Cohen, M. T. Frederick, L. C. Cass, E. A. Weiss, Simultaneous Determination of the Adsorption Constant and the Photoinduced Electron Transfer Rate for a Cds Quantum Dot-Viologen Complex. *J. Am. Chem. Soc.* 133 (2011) 10146-10154.
- [33] A. Boulesbaa, A. Issac, D. Stockwell, Z. Huang, J. Huang, J. Guo, T. Lian, Ultrafast Charge Separation at CdS Quantum Dot/Rhodamine B Molecule Interface. *J. Am. Chem. Soc.* 129 (2007) 15132-15133.
- [34] J. Huang, D. Stockwell, Z. Huang, D. L. Mohler, T. Lian, Photoinduced Ultrafast Electron Transfer from CdSe Quantum Dots to Re-bipyridyl Complexes. *J. Am. Chem. Soc.* 130 (2008) 5632-5633.
- [35] S.-C. Cui, T. Tachikawa, M. Fujitsuka, T. Majima, Solvent-Polarity Dependence of Electron-Transfer Kinetics in a CdSe/ZnS Quantum Dot-Pyromellitimide Conjugate. *J. Phys. Chem. C* 114 (2010) 1217-1225.
- [36] E. S. Shibu, A. Sonoda, Z. Tao, Q. Feng, A. Furube, S. Masuo, L. Wang, N. Tamai, M. Ishikawa, V. Biju, Photofabrication of Fullerene-Shelled Quantum Dots Supramolecular Nanoparticles for Solar Energy Harvesting. *ACS Nano* 6 (2012) 1601-1608.

- [37] C. He, D. J. Weinberg, A. B. Nepomnyashchii, S. Lian, E. A. Weiss, Control of the redox activity of PbS quantum dots by tuning electrostatic interactions at the quantum dot/solvent interface. *J. Am. Chem. Soc.* 138 (2016) 8847-8854.
- [38] K. E. Knowles, M. Malicki, E. A. Weiss, Dual-Time Scale Photoinduced Electron Transfer from PbS Quantum Dots to a Molecular Acceptor. *J. Am. Chem. Soc.* 134 (2012) 12470-12473.
- [39] A. a. O. El-Ballouli, E. Alarousu, M. Bernardi, S. M. Aly, A. P. Lagrow, O. M. Bakr, O. F. Mohammed, Quantum confinement-tunable ultrafast charge transfer at the PbS quantum dot and phenyl-C61-butyrilic acid methyl ester interface. *J. Am. Chem. Soc.* 136 (2014) 6952-6959.
- [40] Y. Yang, W. Rodríguez-Córdoba, T. Lian, Ultrafast Charge Separation and Recombination Dynamics in Lead Sulfide Quantum Dot–Methylene Blue Complexes Probed by Electron and Hole Intraband Transitions. *J. Am. Chem. Soc.* 133 (2011) 9246-9249.
- [41] A. a. O. El-Ballouli, E. Alarousu, A. R. Kirmani, A. Amassian, O. M. Bakr, O. F. Mohammed, Overcoming the Cut-Off Charge Transfer Bandgaps at the PbS Quantum Dot Interface. *Adv. Funct. Mater.* 25 (2015) 7435-7441.
- [42] F. Odobel, L. Le Pleux, Y. Pellegrin, E. Blart, New photovoltaic devices based on the sensitization of p-type semiconductors: challenges and opportunities. *Acc. Chem. Res.* 43 (2010) 1063-1071.
- [43] F. Odobel, Y. Pellegrin, E. A. Gibson, A. Hagfeldt, A. L. Smeigh, L. Hammarström, Recent advances and future directions to optimize the performances of p-type dye-sensitized solar cells. *Coord. Chem. Rev.* 256 (2012) 2414-2423.
- [44] F. Odobel, Y. Pellegrin, Recent advances in the sensitization of wide-band-gap nanostructured p-type semiconductors. Photovoltaic and photocatalytic applications. *J. Phys. Chem. Lett.* 4 (2013) 2551-2564.
- [45] L. Zhang, L. Favereau, Y. Farre, E. Mijangos, Y. Pellegrin, E. Blart, F. Odobel, L. Hammarstrom, Ultrafast and slow charge recombination dynamics of diketopyrrolopyrrole-NiO dye sensitized solar cells. *Phys. Chem. Chem. Phys.* 18 (2016) 18515-18527.
- [46] Y. Farré, L. Zhang, Y. Pellegrin, A. Planchat, E. Blart, M. Boujtita, L. Hammarström, D. Jacquemin, F. Odobel, Second Generation of Diketopyrrolopyrrole Dyes for NiO-Based Dye-Sensitized Solar Cells. *J. Phys. Chem. C* 120 (2016) 7923-7940.
- [47] E. A. Gibson, A. L. Smeigh, L. L. Pleux, J. Fortage, G. Boschloo, E. Blart, Y. Pellegrin, F. Odobel, A. Hagfeldt, L. Hammarström, A p-Type NiO-based Dye-Sensitized Solar Cell with a Voc of 0.35 V. *Angew. Chem. Int. Ed.* 48 (2009) 4402-4405.
- [48] A. Morandera, J. Fortage, T. Edvinsson, L. Le Pleux, E. Blart, G. Boschloo, A. Hagfeldt, L. Hammarström, F. Odobel, Improved Photon-to-Current Conversion Efficiency with a Nanoporous p-Type NiO Electrode by the Use of a Sensitizer-Acceptor Dyad. *J. Phys. Chem. C* 112 (2008) 1721-1728.
- [49] L. Le Pleux, A. L. Smeigh, E. Gibson, Y. Pellegrin, E. Blart, G. Boschloo, A. Hagfeldt, L. Hammarström, F. Odobel, Synthesis, photophysical and photovoltaic investigations of acceptor-functionalized perylene monoimide dyes for nickel oxide p-type dye-sensitized solar cells. *Energy Environ. Sci.* 4 (2011) 2075-2084.
- [50] D. Ameline, S. Diring, Y. Farre, Y. Pellegrin, G. Naponiello, E. Blart, B. Charrier, D. Dini, D. Jacquemin, F. Odobel, Isoindigo derivatives for application in p-type dye sensitized solar cells. *RSC Adv.* 5 (2015) 85530-85539.
- [51] L. Zhang, L. Favereau, Y. Farre, A. Maufroy, Y. Pellegrin, E. Blart, M. Hissler, D. Jacquemin, F. Odobel, L. Hammarstrom, Molecular-structure control of electron transfer dynamics of push-pull porphyrins as sensitizers for NiO based dye sensitized solar cells. *RSC Adv.* 6 (2016) 77184-77194.
- [52] A. H. Ip, S. M. Thon, S. Hoogland, O. Voznyy, D. Zhitomirsky, R. Debnath, L. Levina, L. R. Rollny, G. H. Carey, A. Fischer, K. W. Kemp, I. J. Kramer, Z. Ning, A. J. Labelle, K. W. Chou, A. Amassian, E. H. Sargent, Hybrid passivated colloidal quantum dot solids. *Nat. Nano* 7 (2012) 577-582.
- [53] M. Yuan, M. Liu, E. H. Sargent, Colloidal quantum dot solids for solution-processed solar cells. *Nature Energy* 1 (2016) 16016.
- [54] P. V. Kamat, Quantum Dot Solar Cells. The Next Big Thing in Photovoltaics. *J. Phys. Chem. Lett.* 4 (2013) 908-918.

- [55] P. V. Kamat, K. Tvrdy, D. R. Baker, J. G. Radich, Beyond Photovoltaics: Semiconductor Nanoarchitectures for Liquid-Junction Solar Cells. *Chem. Rev.* 110 (2010) 6664-6688.
- [56] J. Tang, K. W. Kemp, S. Hoogland, K. S. Jeong, H. Liu, L. Levina, M. Furukawa, X. Wang, R. Debnath, D. Cha, K. W. Chou, A. Fischer, A. Amassian, J. B. Asbury, E. H. Sargent, Colloidal-quantum-dot photovoltaics using atomic-ligand passivation. *Nat. Mater.* 10 (2011) 765-771.
- [57] Mahfoudh Raissi, M. T. Sajjad, Y. Pellegrin, T. Roland, S. Jobic, M. Boujtita, A. Ruseckas, I. D. W. Samuel, F. Odobel, Size dependence of efficiency of PbS quantum dots in NiO-based dye sensitised solar cells and mechanistic charge transfer investigation. *Nanoscale* 9 (2017) 15566–15575.
- [58] P. Ho, L. Q. Bao, K.-S. Ahn, R. Cheruku, J. H. Kim, P-Type dye-sensitized solar cells: Enhanced performance with a NiO compact blocking layer. *Synthetic Metals* 217 (2016) 314-321.
- [59] Q. Liu, L. Wei, S. Yuan, X. Ren, Y. Zhao, Z. Wang, M. Zhang, L. Shi, D. Li, The effect of Ni(CH₃COO)₂ post-treatment on the charge dynamics in p-type NiO dye-sensitized solar cells. *J. Mater. Sci.* 50 (2015) 6668-6676.
- [60] N. C. Anderson, M. P. Hendricks, J. J. Choi, J. S. Owen, Ligand Exchange and the Stoichiometry of Metal Chalcogenide Nanocrystals: Spectroscopic Observation of Facile Metal-Carboxylate Displacement and Binding. *J. Am. Chem. Soc.* 135 (2013) 18536-18548.
- [61] A. Pal, S. Srivastava, R. Gupta, S. Sapra, Electron transfer from CdSe-ZnS core-shell quantum dots to cobalt(iii) complexes. *Phys. Chem. Chem. Phys.* 15 (2013) 15888-15895.
- [62] B. Abraham, S. McMasters, M. A. Mullan, L. A. Kelly, Reactivities of Carboxyalkyl-Substituted 1,4,5,8-Naphthalene Diimides in Aqueous Solution. *J. Am. Chem. Soc.* 126 (2004) 4293-4300.
- [63] D. Gosztola, M. P. Niemczyk, W. Svec, A. S. Lukas, M. R. Wasielewski, Excited Doublet States of Electrochemically Generated Aromatic Imide and Diimide Radical Anions *J. Phys. Chem. A.* 104 (2000) 6545-6551.
- [64] E. A. Gibson, A. L. Smeigh, L. Le Pleux, L. Hammarström, F. Odobel, G. Boschloo, A. Hagfeldt, Cobalt Polypyridyl-Based Electrolytes for p-Type Dye-Sensitized Solar Cells. *J. Phys. Chem. C* 115 (2011) 9772-9779.